THE TERGRA MODEL - A MATHEMATICAL MODEL FOR THE SIMULATION

OF THE DAILY BEHAVIOUR OF CROP SURFACE TEMPERATURE

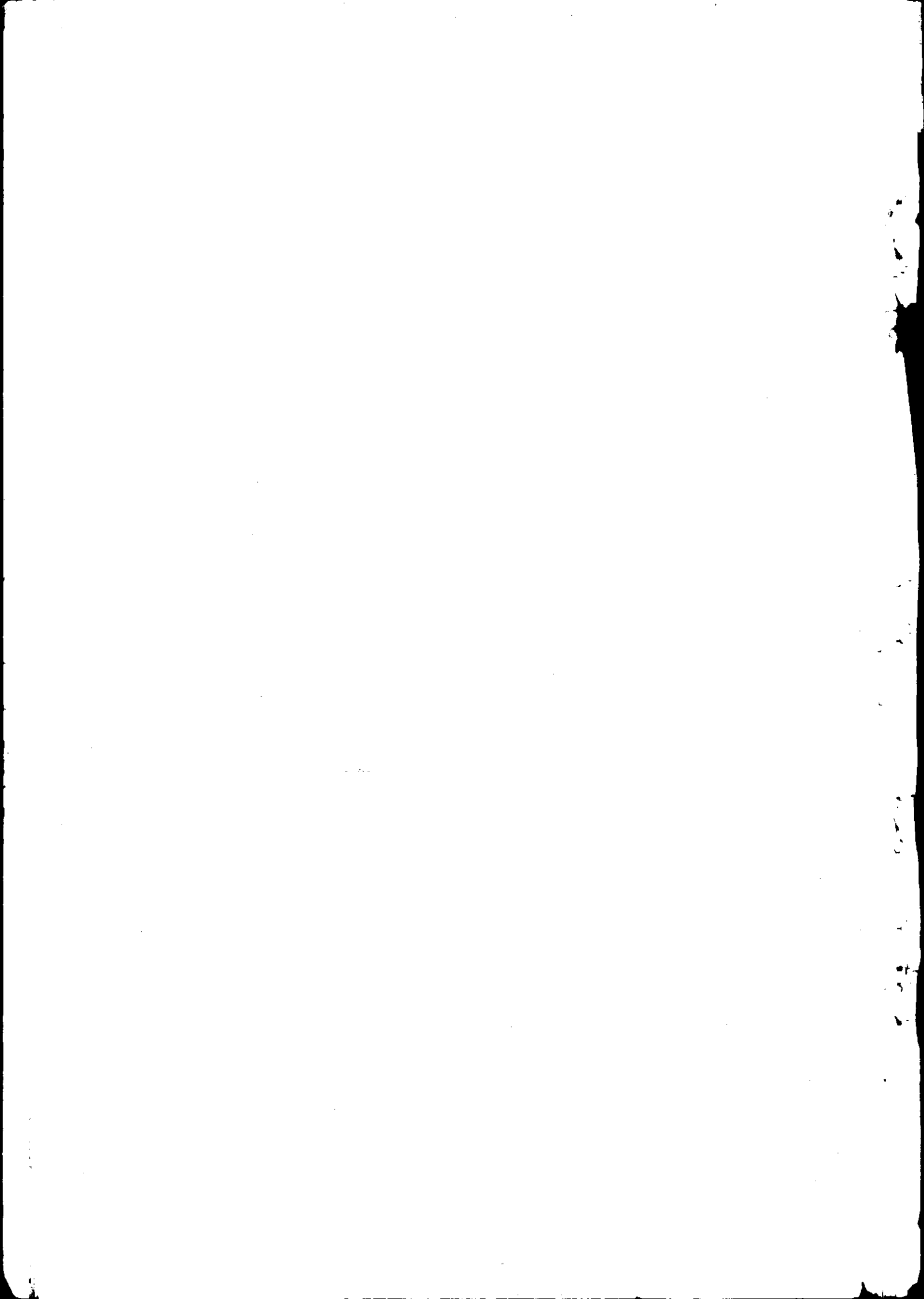## AND ACTUAL EVAPOTRANSPIRATION

ir. G.J.R. Soer

Nota's van het Instituut zijn in principe interne communicatie-
middelen, dus geen officiële publicaties.
Hun inhoud varieert sterk en kan zowel betrekking hebben op een
eenvoudige weergave van cijferreeksen, als op een concluderende
discussie van onderzoeksresultaten. In de meeste gevallen zullen
de conclusies echter van voorlopige aard zijn omdat het onderzoek
nog niet is afgesloten.
Bepaalde nota's komen niet voor verspreiding buiten het Instituut
in aanmerking

ISN 138242-04

C O N T E N T S

PREFACE

This study was effected in the framework of the NIWARS investigations on the application of thermal infrared scanning. It concerns the application of thermal infrared scanning for the measurement of aerial heat and water budgets of cropped surfaces. The study was executed in collaboration with the Department of Hydrology of the Institute for Land and Water Management Research on detachment to this Institute.

The author is indebted to all co-operators of NIWARS and ICW who made the execution of measurements and processing possible.

He expresses his gratitude to Ir. A Rosema en Dr. R.A. Feddes for their permanent support in physical matters.

It was the intention to have this study published as NIWARS publication 46. As the last version was not ready before the premature end of all NIWARS activities, it is published provisionally as a note of the ICW.

LIST OF USED SYMBOLS

Symbol	Description	Units	Symbol in comp. program
b	root density resistance factor	m	RD
c	specific heat per unit mass of soil	$J.kg^{-1}.K^{-1}$	–
c_p	specific heat per unit mass of air	$J.kg^{-1}.K^{-1}$	CP
d	zero plane displacement	m	–
E	evapotranspiration flux	$kg.m^{-2}.s^{-1}$	–
e_a	actual water vapour pressure in the air at height z_a	Pa	EA
e_c^*	saturated water vapour pressure in the air at temperature T_c	Pa	EOS
G	heat flux into the soil	$W.m^{-2}$	GHF
g	acceleration due to gravity	$m.s^{-2}$	G
H	sensible heat flux	$W.m^{-2}$	H
h	crop height	m	GHC
K	unsaturated hydraulic conductivity	$m.s^{-1}$	AK
K_s	saturated hydraulic conductivity	$m.s^{-1}$	AKO
k	Von Karman's constant (k = 0.40)	–	AKAR
L	latent heat of vaporization	$J.kg^{-1}$	ALABDA
m	pore size distribution factor	–	BL
N, n	maximum possible resp. actual duration of sunshine per time interval	s	–
P_1	stability correction for momentum transport	–	PSIONE
P_2	stability correction for heat transport	–	PSITWO
R_1	longwave sky radiation flux	$W.m^{-2}$	RL
R_n	net radiation flux	$W.m^{-2}$	RN
R_o	solar constant	$W.m^{-2}$	–
R_s	incoming shortwave radiation flux	$W.m^{-2}$	RS
r_a	turbulent diffusion resistance for heat and water vapour transport	$s.m^{-1}$	RA

Symbol	Description	Units	Symbol in comp. program
r_c	crop diffusion resistance for water vapour transport	$s.m^{-1}$	RC
r_{pl}	plant resistance for water transport	s	RPL
r_s	stomatal resistance for water vapour transport	$s.m^{-1}$	–
r_{so}	soil hydraulic resistance	s	–
S	saturation of soil with water	–	S
S_r	rest saturation	–	SR
T_a	air temperature at height z_a	K	TPA
T_c	crop temperature at height z_{oh}	K	TPO
u	wind velocity at height z_a	$m.s^{-1}$	U
u_*	friction velocity	$m.s^{-1}$	–
x	non dimensional wind velocity gradient as a function of Λ	–	–
x_{sm}	volume fraction of soil mineral components	–	–
x_{so}	volume fraction of soil organic components	–	SO
x_w	volume fraction of soil water	–	THETA
z_a	reference level in the atmosphere	m	ZR
z_e	effective rooting depth	m	DD
z_o	crop roughness	m	ZO
z_{oh}	crop roughness length for sensible heat	m	–
z_{om}	crop roughness length for momentum	m	–
α_1	reflection coefficient for longwave radiation	–	–
α_m	dummy reflection coefficient at $\beta = 0$	–	REFL
α_s	reflection coefficient for short-wave radiation	–	REFLEC
β	solar elevation	o	SUNEL
γ	psychrometric constant	$Pa.K^{-1}$	GAMMA

2

Symbol	Description	Units	Symbol in comp. program
ε	crop emission coefficient	–	EC
θ	volumetric water content	–	THETA
θ_s	saturated volumetric water content equivalent to pore volume	–	THETAS
Λ	Monin-Obukhov length	m	AMOL
λ	heat conductivity of soil	$W.m^{-1}.K^{-1}$	HC
ρ	density of moist air	$kg.m^{-3}$	RHO
ρ_s	density of soil	$kg.m^{-3}$	D
σ	Stefan-Bolzmann constant ($\sigma = 5.67 \times 10^{-8}$)	$W.m^{-2}.K^{-4}$	–
τ	transmission coefficient of the atmosphere	–	–
		–	–
Ψ_a	air entry value of soil	Pa	PSIA
Ψ_l	leaf water pressure	Pa	PSIL
Ψ_s	soil water pressure	Pa	PSIS
Ψ_t	non-dimensional soil water pressure ($\Psi_t = \Psi_s/\Psi_a$)	–	PSIT

LIST OF SYMBOLS USED IN COMPUTER PROGRAM ONLY

ALE	latent heat flux (= L.E)	$W.m^{-2}$
AMA	molecular weight of dry air (AMA = 0.0289644)	$kg.mol^{-1}$
AMV	molecular weight of water vapour (AMV = 0.0180153)	$kg.mol^{-1}$
CARIS	capillary rise	$m.d^{-1}$
CTST	correction on local time to get true solar time	h
DATE, HOUR, AMIN	beginning time of simulation in day number, hours and minutes	–, h, min
DAYS	length of simulation	d
DECL	declination	o

Symbol	Description	Units
DELT	interval meteorological data	min
DEW	accumulated dew	m
DT	simulation time step	min
ENBA	sum of energy balance components	$W.m^{-2}$
EVAP	evapotranspiration at constant temperature	m
HCD	heat conductivity of dry soil	$W.m^{-1}.K^{-1}$
HCS	heat conductivity of saturated soil	$W.m^{-1}.K^{-1}$
HOAN	hour angle from noon	^{o}
PA	air pressure	Pa
PSIDHC	soil moisture pressure at HCD	Pa
RG	gas constant (RG = 8.31432)	$J.mol^{-1}.K^{-1}$
RHOAIR	density of dry air	$kg.m^{-3}$
RHOC	heat capacity of soil (= $\rho_s c$)	$J.m^{-3}.K^{-1}$
RHOVAP	density of water vapour in air	$kg.m^{-3}$
ROWA	density of water at 20^oC (ROWA=998.2)	$kg.m^{-3}$
SINK	root water uptake from soil	m
SLAT	latitude	^{o}
TPK	zero degree Celcius Kelvin equivalent (TPK = 273.15)	K
TPS	soil temperature	K
TRUEST	true solar time	h
ZONEST	local time	h

4

1. INTRODUCTION

The TERGRA model was developed as an aid for the interpretation
of IRLS images of cropped surfaces, with particular emphasis on grass-
land. The model simulates, under specified meteorological conditions
and for different situations of soil moisture pressure, the daily be-
haviour of crop temperature and energy balance components. It is based
on the transport equations for one dimensional vertical heat and
moisture flow in the soil-plant-atmosphere continuum. Boundary condi-
tions are the temperature and soil moisture pressure at a reference
level in the soil, the energy balance equation at the crop surface,
and the temperature and water vapour pressure at a reference level in
the atmosphere. Some relations between model parameters are introduced
in the model. A numerical algorithm to solve the transport equations
completes the model.

The TERGRA model was tested with data gathered at the Losser
study area. The measurements performed in this study area are mentioned
in NIWARS publication 45 (SOER, 1977).

2. THEORY

2.1. Water and heat transport

2.1.1. Introduction

The flow of water and heat in the soil-plant-atmosphere continuum
can be expressed as a combination of transport equations, with driving
forces and resistances similar to Ohm's law.

Fig. 1 shows the resistance model of water and heat flow used
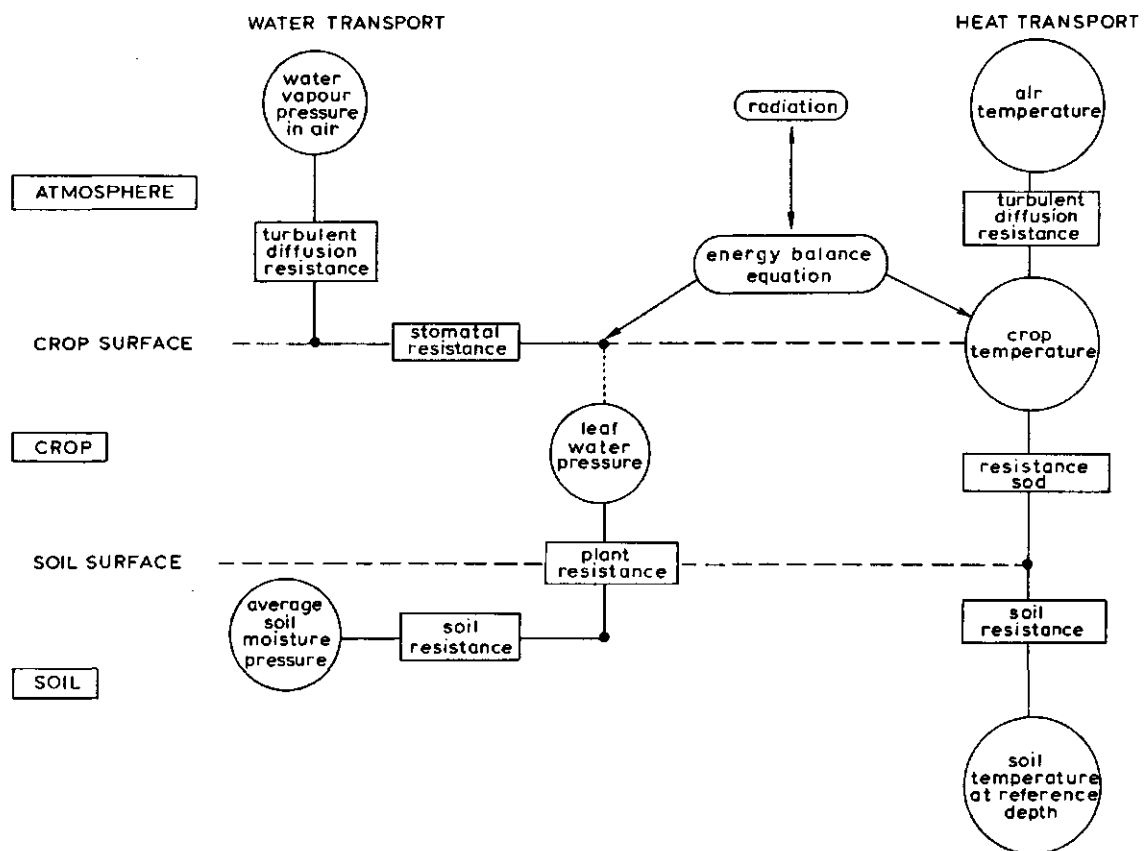in the TERGRA model.

Fig. 1. Resistance model of water and heat flux in the soil-plant-
atmosphere continuum

Under evaporative conditions, water flows from the root zone through the root epidermis, the plant hydraulic system and the stomata to the atmosphere. In the root zone, water flow meets a resistance depending on soil water pressure. The resistances in root epidermis and plant hydraulic system are taken to be constant in this study. The stomatal resistance depends on the opening of the stomata which controls the release of water to the atmosphere.

While water flow is mainly governed by plant physiological factors, heat flow is more passive, depending on the plant's ability to evaporate. Though the heat flow resistances in soil, canopy and atmosphere are variable, they do not influence the heat flow considerably.

2.1.2. Water and heat transport in the atmosphere

Water and heat transport in the atmosphere are mainly passive transport processes, governed both by momentum exchange. Expressing the sensible heat flux and the latent heat flux in the form of transport equations may give:

$$H = \rho \, c_p \frac{T_a - T_c}{r_a} \tag{1}$$

$$L.E = \frac{\rho \, c_p}{\gamma} \cdot \frac{e_a - e_c^*}{r_a + r_c} \tag{2}$$

where H is the sensible heat flux ($W.m^{-2}$), L.E the latent heat flux ($W.m^{-2}$), L the latent heat of vaporization of water ($J.kg^{-1}$), E the evapotranspiration flux ($kg.m^{-2}.s^{-1}$), ρ the density ($kg.m^{-3}$) and c_p the specific heat ($J.kg^{-1}.K^{-1}$) of moist air, γ the psychrometric constant ($Pa.K^{-1}$), T_a the air temperature (K), T_c the crop temperature (K), e_a the water vapour pressure (Pa) in the air, e_c^* the saturated water vapour pressure (Pa) at temperature T_c, r_a the turbulent diffusion resistance for heat and vapour transport ($s.m^{-1}$) and r_c is the crop diffusion resistance for vapour transport ($s.m^{-1}$). It is assumed that the vapour pressure within the stomata equals e_c^* . Fluxes towards the crop surface are taken to be positive.

The turbulent diffusion resistance r_a is a function of the wind velocity u ($m.s^{-1}$), the stability of the atmosphere just above the

crop, and of the nature of the surface (crop height, crop structure). Under conditions of neutral stability ($T_c \simeq T_a$), r_a can be expressed as a function of only wind velocity and roughness of the surface:

$$r_a = \frac{\ln(\frac{z_a-d}{z_{om}}) \; \ln(\frac{z_a-d}{z_{oh}})}{k^2 u} \tag{3}$$

where z_a (m) is an elevation reference level in the atmosphere where wind velocity and air temperature are recorded, d the zero displacement (m), k Von Karman's constant (here taken to be 0.4), z_{om} the roughness length for momentum (m) and z_{oh} the roughness length for sensible heat (m).

When evapotranspiration is reduced crop temperature will rise and unstable conditions will come into being ($T_c > T_a$). Due to temperature induced differences in air density, vertical mass as well as heat transport will increase. For such conditions BUSINGER (1966), BUSINGER et al. (1971) and DYER (1967) derived semi-empirical mass and heat transport formulas (hereafter referred to as the Businger-Dyer concept), based on the use of the Monin-Obukhov length Λ (m) as a measure for stability (MONIN and OBUKHOV, 1954):

$$\Lambda = \frac{u_*^3 \; \rho \; c_p \; T_a}{k \; g \; H} \tag{4}$$

where u_* is the friction velocity (m.s^{-1}) and g is the acceleration due to gravity (9.813 m.s^{-2}). Under unstable conditions r_a can be expressed as (cf. PAULSON, 1971):

$$r_a = \frac{\left[\ln(\frac{z_a-d}{z_{om}}) - P_1\right] \cdot \left[\ln(\frac{z_a-d}{z_{oh}}) - P_2\right]}{k^2 u} \tag{5}$$

where P_1 and P_2 are functions of Λ according to:

$$P_1 = 2 \ln(\frac{1+x}{2}) + \ln(\frac{1+x^2}{2}) - 2 \arctan(x) + \frac{\pi}{2} \tag{6}$$

$$P_2 = 2 \ln(\frac{1+x^2}{2}) \tag{7}$$

where

$$x = (1-16 \; \frac{z_a-d}{\Lambda})^{0.25} \tag{8}$$

Eq. 8 does not hold for extremely unstable conditions when free convection predominates. Practically, for grassland, the Businger-Dyer concept holds for wind velocities of more than about $1 \; m.s^{-1}$ at 2 m height.

For __stable conditions__ ($T_c < T_a$), the formulas established by WEBB (1970) can be used. According to BUSINGER et al. (1971) a value of 4.7 was adopted for the constant in this formulas:

$$r_a = \frac{\left[\ln(\frac{z_a-d}{z_{om}}) + 4.7 \frac{z_a-d}{\Lambda} \right] \cdot \left[\ln(\frac{z_a-d}{z_{oh}}) + 4.7 \frac{z_a-d}{\Lambda} \right]}{k^2 u} \quad \text{for } \Lambda > z_a-d \tag{9}$$

$$r_a = \frac{\left[\ln(\frac{z_a-d}{z_{om}}) + 4.7 \right] \cdot \left[\ln(\frac{z_a-d}{z_{oh}}) + 4.7 \right]}{k^2 u} \quad \text{for } 0 < \Lambda \leqslant z_a-d \tag{10}$$

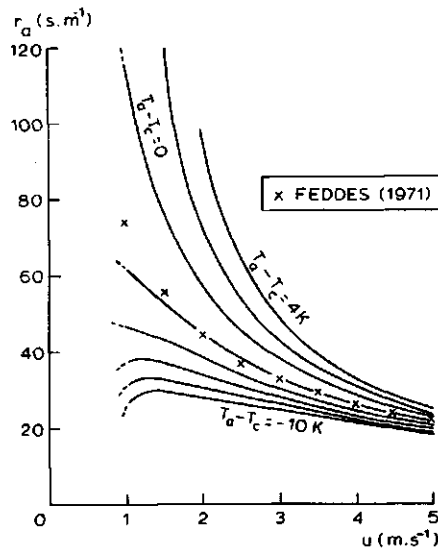Fig. 2. Theoretically derived relation between the turbulent diffusion resistance r_a and wind velocity u for a crop height of 0.20 m, at different air-crop temperature gradients (T_a-T_c). The values are compared with data of FEDDES (1971)

Fig. 2 shows for a crop height of 0.20 m the relation between r_a

and wind velocity for air – crop temperature gradients varying from
–10 to 4 K. The calculations were performed assuming:

$$z_{oh} = z_{om} = z_o \qquad (11)$$

where z_o is the crop roughness (m) which can be calculated from the
crop height h (m) using a simple relation established by MONTEITH
(1973):

$$z_o = 0.13 \, h \qquad (12)$$

The calculated r_a values are compared with values empirically de-
rived by FEDDES (1971). They agree well for high wind velocities. For
low wind velocities the values of Feddes seem to include some instabi-
lity, which agrees with the climatological conditions during which
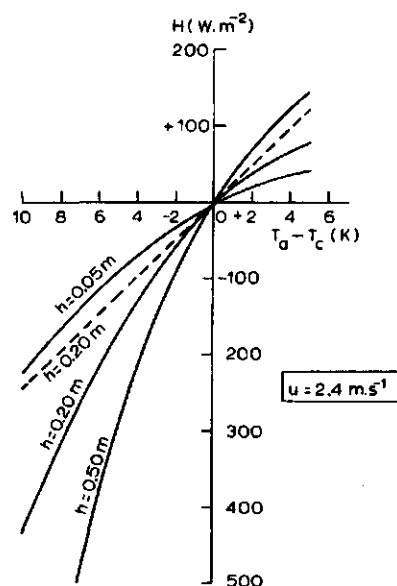those values were derived.

Fig. 3. Theoretically derived relation between sensible heat flux H
and the air – crop temperature gradient $(T_a - T_c)$, for three
different crop heights h at a wind velocity u = 2.4 m.s^{-1}. The
dotted line gives the relation without stability correction
for h = 0.20 m

Using r_a from eqs. 5, 9 and 10 in eq. 1 yields equations in which

the sensible heat flux H depends in a rather complicated way on wind velocity, air - crop temperature gradient and roughness parameters. For unstable conditions these equations can only be solved by iteration techniques (cf. ROSEMA, 1975). Fig. 3 shows such a relation for three different crop heights and a wind velocity of 2.4 $m.s^{-1}$. A simple relation for a crop height of 0.20 m assuming no influence of stability on sensible heat flux and using eq. 3 to calculate r_a is also given in Fig. 3. It appears that neglecting the influence of stability may cause large errors when calculating H.

Recent work (BRUTSAERT, 1977; HEILMAN and KANEMASU, 1976; THOM, 1972) indicates that z_{oh} must be an order of magnitude lower than z_{om} and that it depends not only on the nature of the surface, but also on the nature of the surrounding air. As there is up to now insufficient experimental evidence, eq. 11 is used in the model.

2.1.3. Stomatal resistance

The crop resistance r_c which is part of the total diffusion resistance for water vapour transport, is included in eq. 2. The resistance r_c is the reciprocal sum of the cuticular resistance and the stomatal resistance. As the cuticular resistance is at least one order of magnitude higher than the stomatal resistance, flow through the cuticula can be neglected and the crop resistance r_c can simply be replaced by the stomatal resistance r_s.

Stomatal resistance as a result of closing of the stomata is caused by decreasing water turgor pressure in the guard cells surrounding the stomata. This water turgor pressure is mainly influenced by leaf water pressure and photosynthetic active radiation (PAR). The latter is about 0.5 of the incoming shortwave radiation R_s. By the way of chemical transformations in the leaf cells solution, PAR causes changes in osmotic pressure of the guard cells. This proces is responsible for the closure of stomata when incoming shortwave radiation is low (at night and by day under conditions of low solar elevation or many clouds).

To maintain the water transport from the root zone to the leaf cells, the leaf water pressure must be lower than the soil moisture pressure. Particularly under dry soil conditions this results in

11

very low leaf water pressure values down to -5 MPa (-50 bar). This leaf water pressure influences directly the turgor pressure of the guard cells. Actually the influences of leaf water pressure and PAR on the stomatal closure are coupled in a complicated way. However simple resistance models appear to work satisfactory.

A first attempt to make such a model was made by RIJTEMA (1965). However, as this model was derived for mean daily values it can hardly be used in the TERGRA model. A better approximation for our purpose is the schematic representation of SHAWCROFT et al. (1973), confirmed experimentally by BERGER (1973):

$$r_s = f(\Psi_1) + \frac{a}{R_s + b} \tag{14}$$

where a is an empirical constant derived from measurements, b an empirical constant added to R_s to maintain r_s at some finite level when R_s becomes zero and Ψ_1 the leaf water pressure (Pa).

Little is known about the daily behaviour of r_s of grassland with respect to R_s. However SHAWCROFT et al. (1973), BERGER (1973) and TURNER (1973) for example indicate a hyperbolical relation of the type of eq. 14. For a and b arbitrary values of respectively 400 Pa and 1.5 $W.m^{-2}$ were chosen for the model.

Combining Fig. 36 and Fig. 37 of RIJTEMA (1965) a relation for grassland between r_s and Ψ_1 can be given for $R_s \gg 0$ and a crop cover of 100%. It is estimated from Rijtema that this relation is valid for a mean crop height of 0.14 m:

$$r_s = 4.52 \times 10^{-12} (-\Psi_1)^{2.1} \tag{15}$$

From Fig. 37 of Rijtema it appears that r_s remains constant when Ψ_1 comes above the range -1 to -0.7 MPa (-10 to -7 bar). So the value of -0.7 MPa was accepted as the maximum value of Ψ_1, for which r_s varies with Ψ_1. As a consequence, inserting this value in eq. 15 and 14, the model works with a minimum value for r_s of about 9 $s.m^{-1}$. RIJTEMA (1965) found as a minimum value for $\Psi_1 = -5$ MPa (-50 bar). This value was adopted for the model as an absolute minimum.

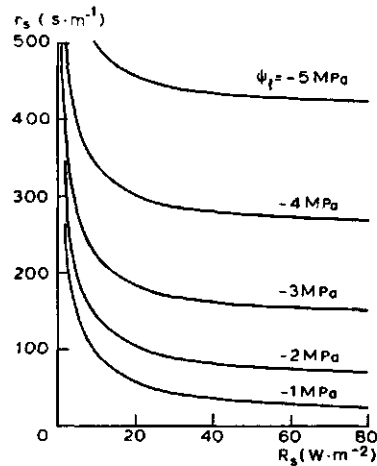All these values are pertaining to a crop height of 0.14 m. As

Fig. 4. Relation between the stomatal resistance r_s and the incoming shortwave radiation flux R_s for different values of leaf water pressure Ψ_1

the number of stomata may vary with crop height, a correction for other crop heights may be needed. As far as is known there is no experimental evidence about this subject. We can make two assumptions:

a) the number of stomata does not change with crop height;

b) the number of stomata varies directly proportional to biomass and, assuming a linear relation between crop height and biomass, to crop height too.

The actual relation is somewhere in between. Arbitrarily r_s was chosen to be inversely proportional to the square root of h. We can write now:

$$r_s = h^{-0.5}(3.2 + \frac{400}{R_s+1.5}) \qquad \text{for } \Psi_1 \geq -0.7 \text{ MPa} \tag{16}$$

$$r_s = h^{-0.5}(1.69\text{x}10^{-12}(-\Psi_1)^{2.1} + \frac{400}{R_s+1.5}) \quad \text{for } -0.7 \text{ MPa} > \Psi_1 > -5 \text{ MPa} \tag{17}$$

$$r_s = h^{-0.5}(197.7 + \frac{400}{R_s+1.5}) \qquad \text{for } \Psi_1 = -5 \text{ MPa} \tag{18}$$

Fig. 4 shows for a crop height of 0.20 m the relation between r_s and R_s for different values of Ψ_1.

2.1.4. Plant and soil resistance to water flow

The evapotranspiration flux E is supposed to be equal to the water flux through soil and plant and can be expressed as (FEDDES and RIJTEMA, 1972):

$$E = \frac{1}{g} \frac{\Psi_1 - \Psi_s}{r_{pl} + r_{so}} \tag{19}$$

where Ψ_s is the soil water pressure (Pa) in the root zone, r_{pl} the plant resistance (s) which is the sum of root epidermis resistance and plant hydraulic resistance and r_{so} is the soil hydraulic resistance (s).

The soil hydraulic resistance r_{so} can be expressed as:

$$r_{so} = b/K(\Psi_s) \tag{20}$$

where b is the root density resistance factor (m) and $K(\Psi_s)$ is the hydraulic conductivity of the soil $(m.s^{-1})$ as a function of Ψ_s. FEDDES and RIJTEMA (1972) proposed for crops with a homogeneous root distribution an empirical relation between b and the effective rooting depth z_e (the depth over which 95% of the total root weight is found):

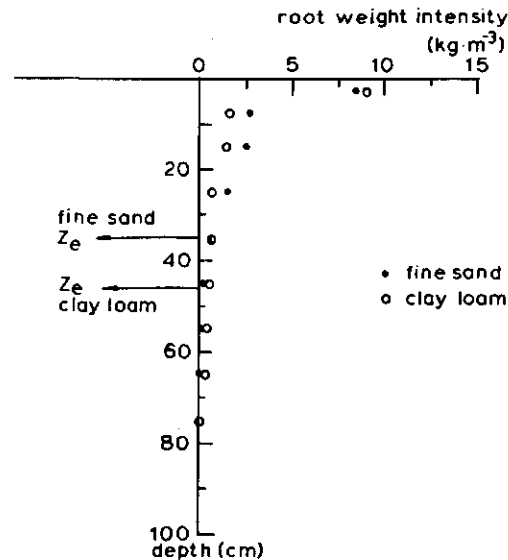$$b = 0.0013 \ z_e^{-1} \tag{21}$$

Fig. 5. Variation of root weight intensity with depth for grass on
fine sand and clay loam. Effective rooting depth z_e

They also indicate that r_{pl} depends in a similar way as b on the root distribution. When this is true, r_{pl} must be directly proportional to b. Taking mean values for r_{pl} and b of RIJTEMA (1965) we can write:

$$r_{pl} = 2.49 \times 10^8 \, z_e^{-1} \qquad (22)$$

However, this description seems to work unsatisfactory. Fig. 5 shows measured values of root weight intensity per depth for fine sand and clay loam respectively. It appears that z_e for fine sand is smaller than for clay loam. Following eqs. 21 and 22 this results in higher b and r_{pl} values for fine sand than for clay loam. In contradiction with this is the total root weight for both soil types, being considerably higher for fine sand. In general it is to be expected that a high total root weight is attended with low resistances. In addition, eq. 22 may give unrealistic low values for r_{pl}.

For these reasons in the TERGRA model, b and r_{pl} were chosen to be directly proportional to the total root weight. To have a reference level b and r_{pl} for fine sand were taken arbitrarily as 3.0 mm and 10 000 d respectively. Table 1 shows the values used for the three main soil types of the Losser area.

Table 1. Soil physical parameters of the three main soil types of the study area

Soil type	b	r_{pl}	K_s	Ψ_a	m
	mm	d	$m.d^{-1}$	kPa	
Fine sand	3.0	10 000	2.0	-2.5	3.38
Clay loam	3.7	12 300	0.01	-2.0	2.39
River deposit	2.4	8 000	0.2	-3.0	3.08

The soil moisture retention curves of the fine sand and the clay loam are presented in Fig. 6. Following LALIBERTE et al. (1968) we can approximate these curves by:

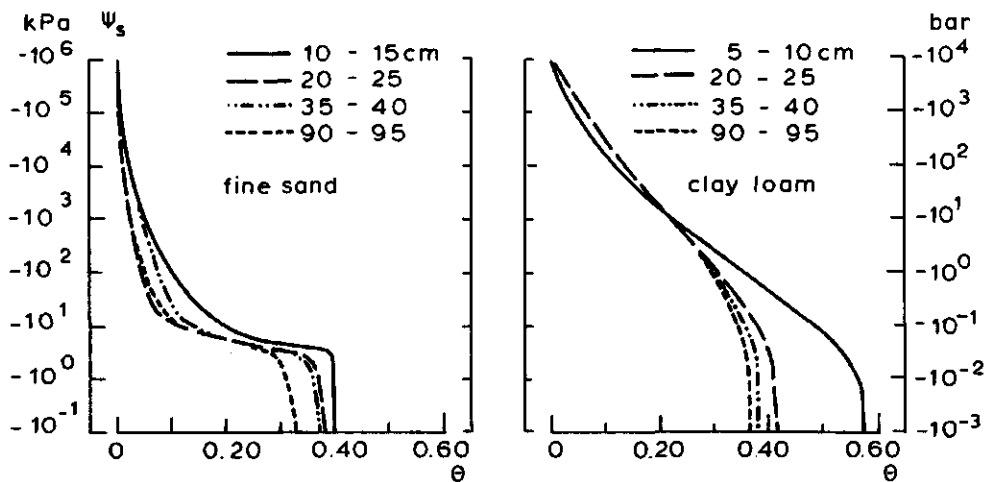$$\frac{S - S_r}{1 - S_r} = \Psi_t^{-m} \qquad (23)$$

Fig. 6. Soil moisture retention curves for fine sand and clay loam
at various sampling depths

where S is the saturation defined as θ/θ_s and where θ and θ_s are the
actual and saturated volumetric water content respectively. S_r is the
residual saturation (saturation at which K = 0), Ψ_t equals Ψ_s/Ψ_a,
where Ψ_a is the air entry value (Pa); m is the pore size distribution
factor. Values of Ψ_a and m can be derived from a linear regression
of $\log\left[(S - S_r)/(1 - S_r)\right]$ on $\log(\Psi_t)$. According to BROOKS and COREY
(1964) the K-Ψ_s relation can then be expressed as:

$$K = K_s \cdot \Psi_t^{-(2+3\ m)} \qquad \text{for} \qquad \Psi_t \geqslant 1 \qquad (24)$$

where K_s is the saturated hydraulic conductivity (m.s^{-1}). K_s was
measured in the laboratory at undisturbed soil samples. For the
values of K_s, Ψ_a and m see table 1. The so calculated K - Ψ_s-relations
are shown in fig. 7. For $\Psi_s > \Psi_a$, K = K_s.

2.1.5. Heat transport in the soil

The transport of heat into the soil can be expressed as:

$$G = - \lambda \frac{\partial T}{\partial z} \qquad (25)$$

where G is the heat flux into the soil (W.m^{-2}), λ the thermal conduc-
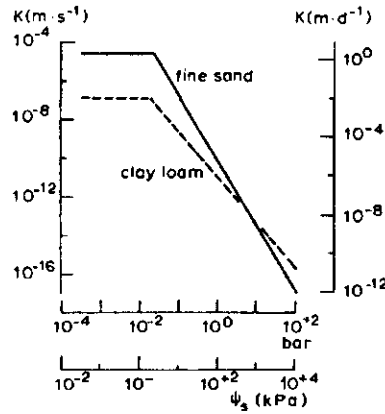tivity (W.m^{-1}.K^{-1}), T the temperature (K) and z the depth (m). The

16

Fig. 7. Relation between the unsaturated hydraulic conductivity K and the soil moisture pressure Ψ_s for fine sand and clay loam as calculated with eq. 24

principle of continuity requires:

$$\frac{\partial G}{\partial z} = -\rho_s \, c \, \frac{\partial T}{\partial t} \tag{26}$$

where ρ_s is the density of the soil (kg.m^{-3}) and c is the specific heat (J.kg^{-1}.K^{-1}). Combining eqs. 23 and 24 gives:

$$\frac{\partial}{\partial z}(\lambda \, \frac{\partial T}{\partial z}) = \rho_s c \frac{\partial T}{\partial t} \tag{27}$$

In the model, this equation is solved with an explicit finite difference scheme (see chapter 3).

The product $\rho_s c$ is called the heat capacity (J.m^{-3}.K^{-1}) and can be expressed as (DE VRIES, 1975):

$$\rho_s c = 10^6 (2 \, x_{sm} + 2.5 \, x_{so} + 4.2 \, x_w) \tag{28}$$

where x_{sm}, x_{so} and x_w are the volume fractions of the soil mineral components, the soil organic components and of the soil water respectively. The volume fraction of soil water x_w is identical with the volumetric water content θ. Using the linear relation   of eq. 28 $\rho_s c$ values were calculated for the fine sand and the clay loam (fig. 8).
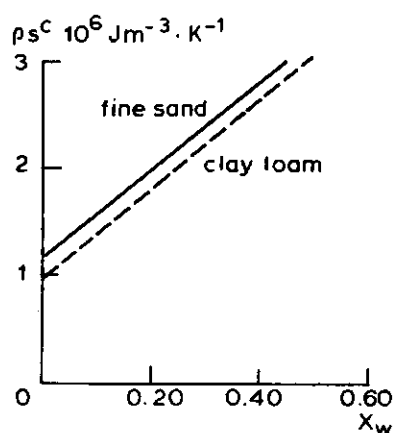
Fig. 8. Relation between the soil heat capacity $\rho_s c$ and the volume
fraction of water x_w for fine sand and clay loam

The thermal conductivity λ can be expressed as a function of the structure of the soil by considering the volume fractions, the geometry and the specific conductivities of its components (DE VRIES, 1952). According to this method, being also explained in NIWARS publication 11 (ROSEMA, 1975), λ values are calculated at different soil moisture contents for the top 10 cm layer of the fine sand and the clay loam (fig 9a). Comparison of these values with experimental data shows a good agreement for dry and saturated soil. In between, particularly at low water contents there is a rather large deviation.

Fig. 9b shows the measured λ values plotted against log (Ψ_s). As no measurements of Ψ_s were made, Ψ_s was derived from θ, using eq. 23. For the curves of fig. 6, a multiple regression was made for each soil separately of respectively Ψ_a and m on soil density and soil organic matter content. Inserting the measured values of soil density and soil organic matter content of the soil samples used for the determination of λ, yields the appropriate values of Ψ_a and m. For λ at saturation and at dry soil, the values calculated with the method of DE VRIES were used as a upper and lower limit. The points for both soil types fit a straight line extremely well. When compared with results of FEDDES (1971) too, it appears that there exists a relation between the slope of the $\lambda - \Psi_s$ curves and the pore size distribution factor m. However, the number of soil types was too small to decide for a generally valid relation. The relations of
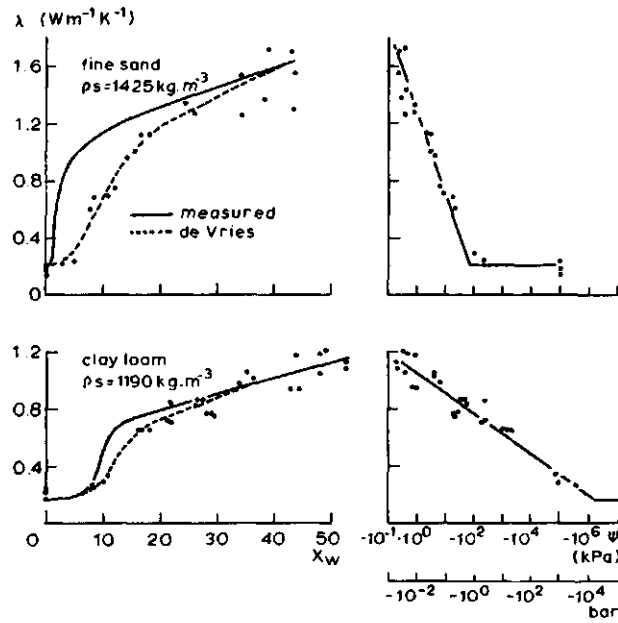
18

Fig. 9. a. Relation between heat conductivity λ and the volume frac-
        tion of water x_w for fine sand and clay loam. The measured
        values are compared with theoretical values according to
        DE VRIES (1952)
     b. Relation between λ and the logarithm of soil moisture
        pressure ψ_s

fig. 9b are used in the model.

2.2. B o u n d a r y   c o n d i t i o n s

2.2.1. Introduction

To solve the transport equations for heat and water flow from
the soil to the atmosphere, boundary conditions are needed(fig. 1).
For water flow, the boundary conditions are the water potentials at
a reference level in the soil and the atmosphere. The water poten-
tials in this study are expressed as potentials per unit volume,
thus equivalent to pressure. For heat flow, the boundary conditions
are the temperatures at some reference level in the soil and in the
atmosphere. As the model is dynamic, the boundary conditions must
also be dynamic, except those which are constant in time.

If the temperature of the evaporating surface has to be known, which is the goal of the model, a supplementary boundary condition has to be introduced in the form of the energy balance equation at this surface.

2.2.2. Boundary conditions in the atmosphere

The boundary conditions in the atmosphere are the temperature and the vapour pressure at some reference level. In this study the reference level was taken at 2 m above the soil surface. However, any other height can be introduced, provided that the temperature and the water vapour pressure are both measured at that height.

The atmospherical boundary conditions are dynamic. They are introduced in the model as mean measured values over discrete time periods or as discrete measurements at certain intervals. Though the model will work with any length of time period, it is recommended to use maximum time periods of 1 hour, making linear interpolation possible. It will not serve to use time periods smaller than 2 min, as the model's sensitivity is not appropriate to it.

2.2.3. Boundary conditions in the soil

The boundary condition for water transport is the soil moisture pressure Ψ_s taken as a mean value for z_e. The boundary condition for heat transport is the temperature at some reference level in the soil where the daily amplitude of temperature is supposed to be zero. In this study this depth was taken to be 0.30 m. As a consequence of the definition of the boundary condition for heat transport, this boundary condition will be constant over the simulation period.

Because of the evapotranspiration the water content of the soil will change during the simulation period and consequently the boundary condition for water flow Ψ_s will change too. This change depends on simulation results and is automatically calculated by the model.

For heat transport, it is also possible to take as boundary condition a constant flux at the reference depth. This might be useful when the soil is cooling down or heating up continously for longer periods. In the model simulations shown in this report, the latter method was used, although it was found that results were quite similar

20

using any type of boundary condition or another.

2.2.4. The energy balance equation

The energy balance equation at the crop surface can be expressed as:

$$R_n + G + H + L \cdot E = 0 \tag{29}$$

where R_n is the net radiation flux $(W.m^{-2})$. Energy used for photosynthetic processes is neglected. Changes in heat storage in the crop, being also part of the energy balance equation, are relatively small for grassland and are left out of account.

2.2.5. The radiation equation

The net radiation flux R_n is the sum of incoming and outgoing radiation components:

$$R_n = (1 - \alpha_s) R_s + (1 - \alpha_1) R_1 - \varepsilon\sigma T_c^4 \tag{30}$$

where α_s and α_1 are the crop's reflection coefficients for shortwave radiation and for longwave radiation respectively, R_1 is the longwave sky radiation flux $(W.m^{-2})$, ε the crop's emission coefficient and σ the Stefan-Boltzmann constant $(5.67 \times 10^{-8} W.m^{-2}.K^{-4})$. As $(1 - \alpha_1) = \varepsilon$, eq. 30 can be rewritten as:

$$R_n = (1 - \alpha_s) R_s + \varepsilon(R_1 - \sigma T_c^4) \tag{31}$$

Either measured or calculated values of R_n may be used as input in the model. As the behaviour of T_c depends on soil moisture pressure, the behaviour of R_n will depend on soil moisture pressure too. This implies that measured R_n values are only valid for one specific soil moisture pressure level. Due to variation of T_c, the variation of R_n at different soil moisture pressure levels may be as large as 90 $W.m^{-2}$, being about 20% of the maximum possible R_n. As the model simulates for different levels of soil moisture pressure, it is prefered to calculate R_n from the measured or estimated parameters at

the right hand side of eq. 31.

S h o r t w a v e   r a d i a t i o n   f l u x. Usually measured R_s
values will be introduced in the model. When the daily course of R_s
is not measured, it is possible to simulate R_s for the whole day.
This is true if during the day the atmospheric transmissivity does
not change and if at least one R_s value is measured around the middle
of the day. Following the calculation method of table 135 and 136 of
the SMITHSONIAN METEOROLOGICAL TABLES (1968) we may write:

$$R_s = 0.5\ R_o\ \sin(\beta)\ (\tau^{\mathrm{cosec}(\beta)} + 0.87) \qquad (32)$$

where R_o is the solar constant (1309 $W.m^{-2}$), β the solar elevation
(see chapter 3.2) and τ is the transmission coefficient of the atmos-
phere. With the aid of eq. 32 R_s values at half hour intervals were
calculated for 29 June 1976 and a comparison was made with measured
values (fig. 10). The agreement is rather good. Values before and
after 1200 true solar time are indicated separately. They show a
small but systematic difference, being probably due to differences
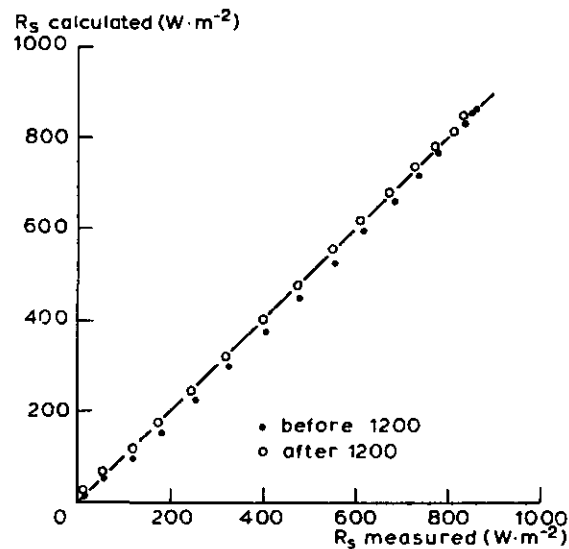in the part of diffuse radiation in R_s.

Fig. 10. Comparison between calculated and measured values of the
incoming shortwave radiation flux R_s. Values before and
after 1200 are indicated separately

S h o r t w a v e   r e f l e c t i o n   c o e f f i c i e n t. The
shortwave reflection coefficient α_s is the weighed sum of the reflec-
tion coefficients of the various wavelengths. In principle these re-
flection coefficients behave different for variations in crop struc-
ture and solar radiation structure. Analyzing grassland spectral
characteristics measured by BUNNIK (pers. comm.), it was found that
α_s can be calculated from a linear relation with near-infrared reflec-
tion as presented by the reflection at 0.81 μm $(\alpha_{0.81})$ (fig. 11),
with an accuracy of 0.006. Considering this result, the behaviour of
α_s can be regarded as being almost identical to the behaviour of
$\alpha_{0.81}$.
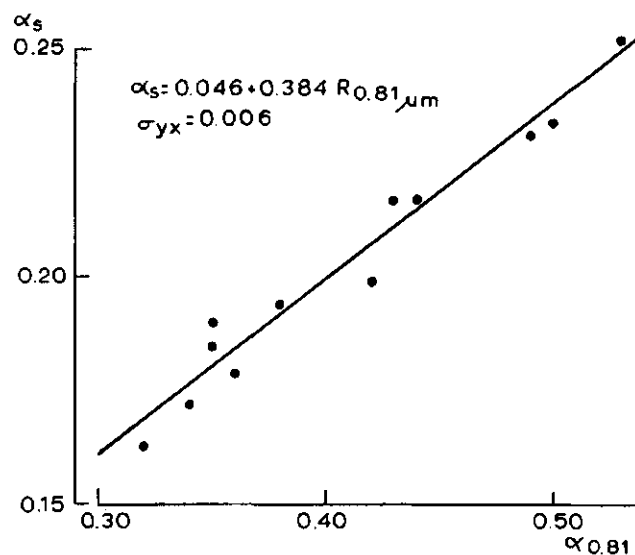
Fig. 11. Relation between the shortwave reflection coefficient α_s
and the reflectance at 0.81 μm $\alpha_{0.81}$

ROSS (1975) established for the reflection of direct solar radia-
tion a formula of the expression:

$$\alpha_s = \frac{\alpha_m}{1 + b \sin(\beta)} \qquad (33)$$

where α_m is a dummy reflection coefficient for $\beta = 0$ and b a constant
depending on crop structure. Figs. 12 and 13 show for grasland the
measured diurnal variation of α_s with local time and with solar ele-
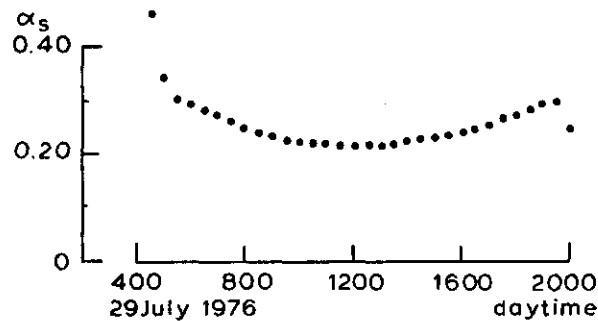
Fig. 12. Measured diurnal variation of the shortwave reflection
coefficient α_s with local time
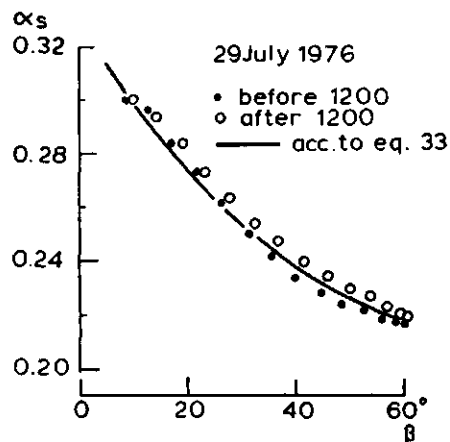
Fig. 13. Measured diurnal variation of α_s with solar elevation
Values before and after 1200 are indicated separately

vation respectively. The behaviour of α_s agrees well with experimental
data of KALMA and BADHAM (1972) and of RIPLEY and REDMANN (1975). The
line through the points of fig. 13 was calculated with eq. 33 using
α_m = 0.33 and b = 0.6. The agreement is good, so it was decided to
use eq. 33 for the total (direct + diffuse) solar radiation.

L o n g w a v e   s k y   r a d i a t i o n. Under no-cloud conditions,
R_1 is a function of air temperature and of humidity. A review on a
number of empirical relations satisfying this dependence was given by
DE JONG (1973). One of the most widely used relations is that of
BRUNT (1939):

$$R_1 = \sigma T_a^4 (a + b\sqrt{e_a}) \tag{34}$$

24

where a and b are empirical constants. For 30 June 1976 a linear regression was made of measured values of R_1 on measured values of T_a and e_a, yielding 0.63 and 0.0046 for a and b respectively. However, it appears also from this regression that the relation between R_1 and e_a is not significant for the daily behaviour of R_1. Repeating this regression only on T_a yields for 'a' a value of 0.80, so:

$$R_1 = 0.80 \; \sigma T_a^4 \tag{35}$$

Plotting the deviation of measured values of R_1 from values calculated with eq. 35 gives fig. 14. The deviation of eq. 35 is small at night and can be considerable by day. Regarding these results, it is highly recommended to use measured values of R_1 in the model, and if measured values are not available, to correct calculated R_1 values according to fig. 14.
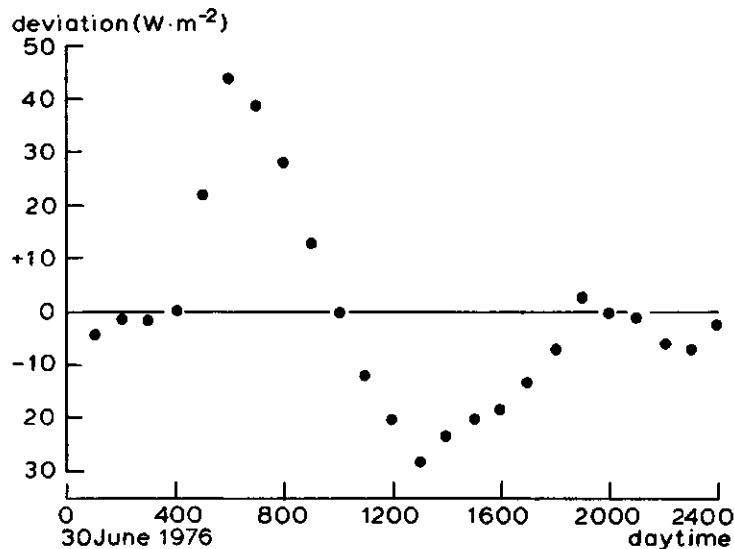

Fig. 14. Deviation of measure values of longwave sky radiation R_1 from values calculated with eq. 35

For cloudy conditions eq. 35 can be expressed as (e.g. FEDDES, 1971):

$$R_1 = \sigma T_a^4 (1 - (1 - a) \frac{n}{N}) \tag{36}$$

25

where n/N is the fraction of clear sky. At this expression has been derived for mean daily values of n/N, it might be questioned if this equation is applicable for the daily behaviour of R_l. As far as is known there is no experimental evidence. It emphasizes once more the importance of using measured values of R_l.

E m i s s i o n   c o e f f i c i e n t. Although it is known that the emission coefficient ε may vary slightly with crop structure, the emission coefficient in the model is taken to be 0.95 for all conditions, as adequate measurements are lacking.

R a d i a t i o n   b a l a n c e. Fig. 15 shows the daily behaviour of measured values of R_l, R_s, σT_c^4, $\alpha_s R_s$ and R_n for 30 June 1976. Longwave radiation does not vary much over the day. At night, shortwave radiation components are absent, while by day the importance of shortwave radiation exceeds that of longwave radiation.
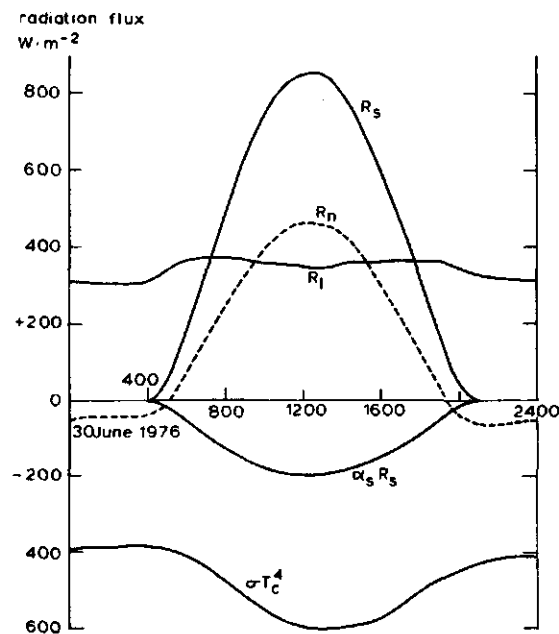

Fig. 15. Daily behaviour of the radiation balance components long-
wave sky radiation R_l, incoming shortwave radiation R_s,
out going longwave radiation $\varepsilon \sigma T_c^4$, reflected shortwave
radiation $\alpha_s R_s$ and net radiation R_n for 30 June 1976

3. COMPUTER PROGRAM

The program is written in Fortran. Fig. 16 gives a flow diagram of the computer program. Appendix I shows the program. Table 2 and table 3 show the input and output parameters respectively with their symbols as used in the report and in the computer program and with the units in which they are introduced in the program.

The most important algorithms are explained in this chapter.

3.1. Iteration procedure

In the program, for each time step, the energy balance components are calculated, starting from the known crop surface temperature TPO at the previous time step. The program checks if the energy balance equation equals zero, if not, a new TPO value is inserted.

Measurements at the test-site indicate that the maximum occurring change in crop surface temperature is about 0.5 $K.min^{-1}$ for moving averages of 20 min and under various weather conditions. From this maximum change the limits between which the new crop surface temperature may vary can be computed as:

$(TPO(t) - 0.5 * DT) \leqslant TPO(t + 1) \leqslant (TPO(t) + 0.5 * DT)$

where t is the number of the time step and DT is the time step. The expression $(TPO(t) - 0.5 * DT)$ is called TPL and $(TPO(t) + 0.5 * DT)$ is denoted TPR. When for a given $TPO(t + 1)$ value the energy balance equation $\neq 0$, a new $TPO(t + 1)$ value is calculated according to Bolzano's method:

IF(ENBA.GT.0.) TPL = $TPO^n(t + 1)$

IF(ENBA.LT.0.) TPR = $TPO^n(t + 1)$

$TPO^{n+1}(t + 1) = \frac{1}{2}(TPL + TPR)$

where ENBA is the sum of the energy balance components and n is the iteration step. The search for the correct $TPO(t + 1)$ value stops when the absolute value of ENBA becomes smaller than 0.5 $W.m^{-2}$.
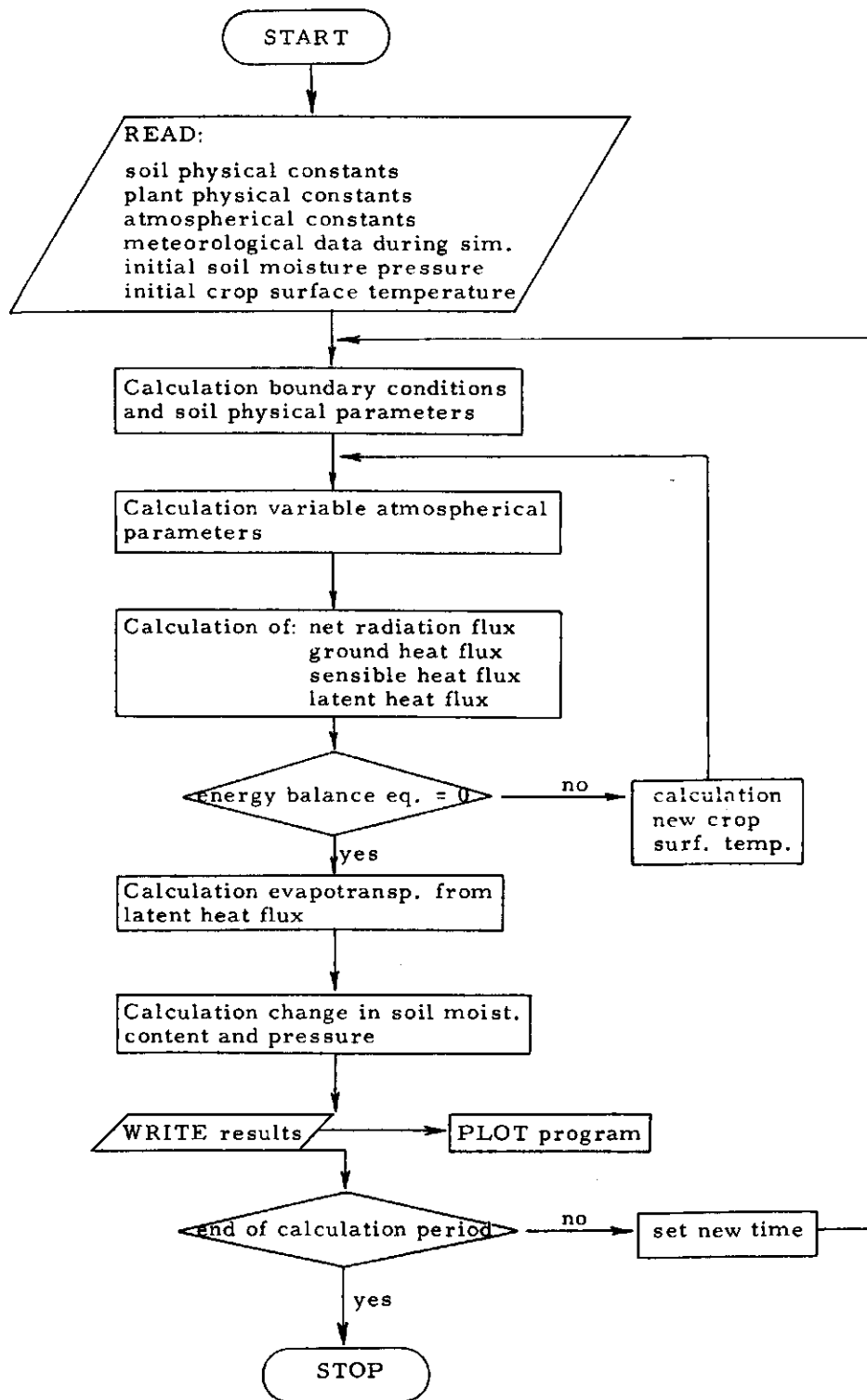
Fig. 16. Flow diagram of the TERGRA model

Table 2. Input parameters

Parameter description	Symbol	Units
Day, hour and minute at begin run	DATE, HOUR, AMIN	-, h, min
Interval meteorological data	DELT	min
Simulation time step	DT	min
Duration simulation	DAYS	d
Acceleration due to gravity	G	$m.s^{-2}$
Initial soil temperature profile	TPS(J)	K
Initial soil moisture pressure	PSIS	kPa
Pore volume	THETAS	-
Exponent $\Psi_s-\theta$ relation	BL	-
Rest saturation	SR	-
Soil density	D	$kg.dm^{-3}$
Soil organic matter fraction	SO	-
Saturated hydraulic conductivity	AKO	$m.d^{-1}$
Air entry value	PSIA	kPa
Heat conductivity at saturated soil	HCS	$W.m^{-1}.K^{-1}$
Heat conductivity at dry soil	HCD	$W.m^{-1}.K^{-1}$
Soil water pressure at HCD	PSIDHC	kPa
Capillary rise	CARIS	$m.d^{-1}$
Global crop height	GHC	m
Plant resistance	RPL	d
Root density resistance factor	RD	mm
Effective rooting depth	DD	m
Dummy reflection coefficient at $\beta = 0$	REFL	-
Emission coefficient	EC	-
Initial value crop temperature	TPO	K
Mean air pressure during simulation	PA	Pa
Correction for true solar time	CTST	h
Latitude	SLAT	o
Declination	DECL	o
Reference height atmospheric measurements	ZR	m
Incoming shortwave radiation flux	RS	$W.m^{-2}$
Incoming longwave radiation flux	RL	$W.m^{-2}$
Air temperature at ZA	TPA	K
Water vapour pressure at ZA	EA	Pa
Wind velocity at ZA	U	$m.s^{-1}$

Table 3. Output parameters

Parameter description	Symbol	Units
Net radiation flux	RN	$W.m^{-2}$
Heat flux into the soil	GHF	$W.m^{-2}$
Sensible heat flux	H	$W.m^{-2}$
Latent heat flux	ALE	$W.m^{-2}$
Crop temperature	TPO	K
Leaf water pressure	PSIL	Pa
Turbulent diffusion resistance	RA	$s.m^{-1}$
Crop diffusion resistance	RC	$s.m^{-1}$
Monin-Obukhov length	AMOL	m
Dew accumulation	DEW	m

This simple iteration procedure appears to work satisfactory under all conditions, as the energy balance equation is a monotoneously increasing function of TPO.

3.2. C a l c u l a t i o n o f n e t r a d i a t i o n

R_n is calculated with the aid of eq. 31 as:

RNI = (1. - REFLEC) * RSI + RLI - RLO

where REFLEC = α_s and RLO = $\varepsilon\sigma T_c^4$. REFLEC is calculated with eq. 33 from the solar elevation SUNEL:

REFLEC = REFL/(1. + 0.6 * SIND(SUNEL))

where REFL = α_m. SUNEL can be expressed as a function of latitude SLAT, declination DECL and hour angle HOAN:

SUNEL = 57.296 * (ASIN(SIND(SLAT) * SIND(DECL) + COSD(SLAT) *

COSD(DECL) * COSD(HOAN))

where:

HOAN = (true solar time - 1200)/100 * 15°

30

3.3. Calculation of heat flux into the soil

The heat flux into the soil G is calculated according to eq. 27, using an explicit finite difference scheme. For that the soil above the reference level of 0.30 m is divided into 15 compartments of 0.02 m each. This gives a regular grid with nodes at the interfaces of the compartments. The nodes are numbered -1 to 16, where -1 is the crop surface, 0 the soil surface and 16 the soil at 0.30 m depth. The separation of soil surface and crop surface was made in order to introduce an empirical resistance that accounts for the isolating effect of the sod. To establish a value for this resistance, simulations were executed at different soil moisture pressures, taking various values for the resistance. It appears that a good fit of measured and simulated soil temperatures is found when $\lambda/\rho_s c$ between nodes -1 and 0 is set equal to one quarter of its value in the soil.

In this way, new soil temperatures are calculated for each node. The heat flux into the soil G is now calculated as the sum for node 0 to 16 of the product of change in soil temperature, heat capacity and depth interval length.

3.4. Calculation of the turbulent diffusion resistance

In chapter 2.1.2 it was stated that r_a for unstable conditions only can be calculated using an iteration procedure. Accepting a small loss of accuracy, a simple calculation procedure without iteration is developed for the model. This concept is only valid for $\Lambda < -1.5$ m.

The wind velocity u can be expressed as (PAULSON, 1971):

$$u = \frac{u_*}{k}\left[\ln\left(\frac{z_a - d}{z_{om}}\right) - P_1\right] \tag{37}$$

and H can be expressed as:

$$H = \frac{\rho \, c_p \, k \, u_*(T_a - T_c)}{\ln(\frac{z_a - d}{z_{oh}}) - P_2} \tag{38}$$

Substituting eqs. 37 and 38 in eq. 4 gives:

$$\Lambda = \frac{T_a \, u^2}{g(T_a - T_c)} \cdot \frac{\ln(\frac{z_a - d}{z_{oh}}) - P_2}{\left[\ln(\frac{z_a - d}{z_{om}}) - P_1\right]^2} \tag{39}$$

It appears that for $z_{oh} = z_{om} = z_o$ and for $\Lambda < -1.5$ m that:

$$\frac{\ln(\frac{z_a - d}{z_{oh}}) - P_2}{\left[\ln(\frac{z_a - d}{z_{om}}) - P_1\right]^2} \simeq \frac{1}{\ln(\frac{z_a - d}{z_o})} \tag{40}$$

with a maximum deviation in r_a of about 1%. Using this relation, Λ and r_a can be calculated directly if T_c is known.

(Remark: This simplification is not allowed when $z_{oh} \neq z_{om} = z_o$).

3.5. Calculation of crop diffusion resistance

Combining eq. 19 with the energy balance equation 29, the leaf water pressure can be calculated from the energy balance components known at the moment. The crop diffusion resistance r_c can then be calculated from the relations of eqs. 16, 17 and 18.

3.6. Calculation of saturated water vapour pressure

ROSEMA (1975) gives a theoretically derived equation for the relation between the vapour density ρ_v and the temperature of water vapour and its matrix pressure Ψ. Taking free water ($\Psi = 0$) and the water vapour pressure e instead of ρ_v, this formula transforms into:

$$e^* = \bar{e}(\frac{T}{\bar{T}})^{\frac{M_v \cdot A}{R}} \cdot \exp\left\{\frac{M_v}{R}(\frac{\bar{L} - A\bar{T}}{\bar{T}} - \frac{\bar{L} - AT}{T})\right\} \tag{41}$$

where $\bar{T}$ is a reference temperature, $\bar{e}$ is the saturated water vapour pressure at $\bar{T}$, $\bar{L}$ the latent heat of vaporization at $\bar{T}$ and A is a coefficient in:

$$L = \bar{L} + A(T - \bar{T}) \tag{42}$$

Putting $\bar{T}$ = 273.15 K, $\bar{e}$ = 610.7 Pa, $\bar{L}$ = 2.501 x 10^6 J.kg^{-1} and A = -2200 J.kg^{-1}.K^{-1}, gives:

$$e^* = 610.7(\frac{273.15}{T})^{4.76696} \cdot \exp(24.606487 \frac{T - 273.15}{T}) \tag{43}$$

The values calculated with eq. 43 were compared with the values of table A.4 of MONTEITH (1973). There is no difference for $0 \leqslant T \leqslant 40^oC$.

3.7. Calculation of dew

At the crop surface, dew formation by condensation of water vapour occurs when L.E is positive. The accumulated dew evaporates at the beginning of the day. As long as dew occurs, r_c is assumed equal to zero and there is no transport of water in plant and soil. This results also in a leaf water pressure being equal to the soil water pressure.

3.8. Calculation of new values of soil moisture pressure

In this part of the model the soil water balance is introduced. The sum of water uptake by the roots SINK and the capillary rise CARIS must equal the change in soil moisture content THETA. Putting the appropriate dimensions, this yields in the program:

THETA = THETA + SINK + CARIS/DD*DT/1440

where DD is the depth of the root zone (= z_e).

From this THETA a new Ψ_s value is calculated using eq. 23 and the parameters of table 1.

4. RESULTS

Many simulations have been carried out with the model. For the sake of simplicity only the simulations executed for 8 July 1975 for the fine sand and a crop height of 0.10 m are shown here. These simulations were performed under conditions of potential evapotranspiration at Ψ_s = -2.5 kPa (-25 mbar) (hereafter refered to as 'wet soil'), giving figs. 17a, b and c. They were also performed for Ψ_s = -350 kPa (-3.5 bar) (hereafter refered to as 'dry soil'), giving figs. 18 a, b and c. Table 4 and 5 give model in- and output parameters for 2-hours intervals for wet and dry soil respectively.

Fig. 17a shows the input parameters wind velocity (U), water vapour pressure (EA) and air temperature (TA) and the output parameter crop temperature (TO).

Fig. 18a shows these parameters for dry soil. In fig. 18a the simulated crop temperatures are compared with crop temperatures measured with a Heimann K24 radiation thermometer (heavy points). It appears that measured and simulated values agree well, except for a small systematic deviation over the whole day, being about 1 K. One possible explanation may be a calibration error of the Heimann radiation thermometer. Another explanation may be that the real emission coefficient does not equal 0.95. A deviation of 0.01 in the emission coefficient results in a deviation of 0.8 K in the crop temperature. Actually these two possible errors are integrated, as the calibration of the radiation thermometer depends mainly on the choice of correct emission coefficients for crop and calibration black body.

By day the crop temperatures at wet soil equal the air temperatures, except for the afternoon when clouds occur. At dry soil the crop temperatures are up to 7 K higher than the air temperatures. In the afternoon the crop temperatures do not differ so much from those simulated at wet soil.
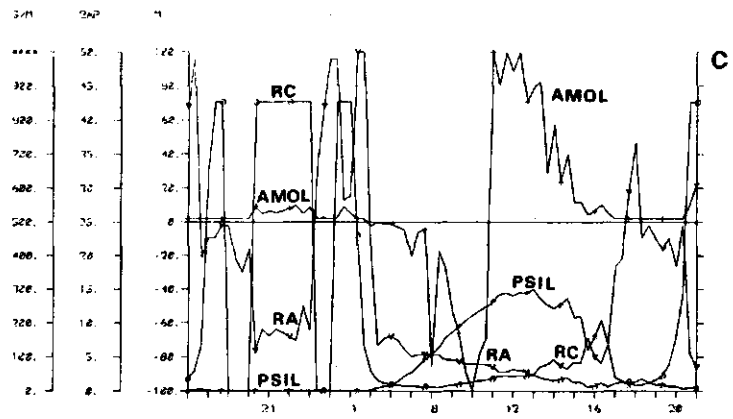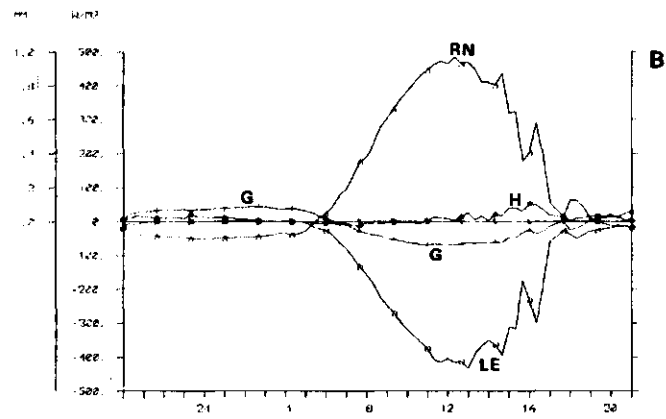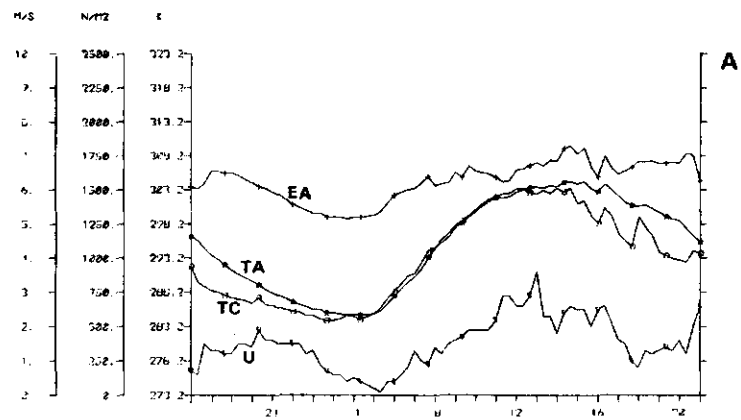

34

Fig. 17a, b and c. Model output for Ψ_s = -2.5 kPa
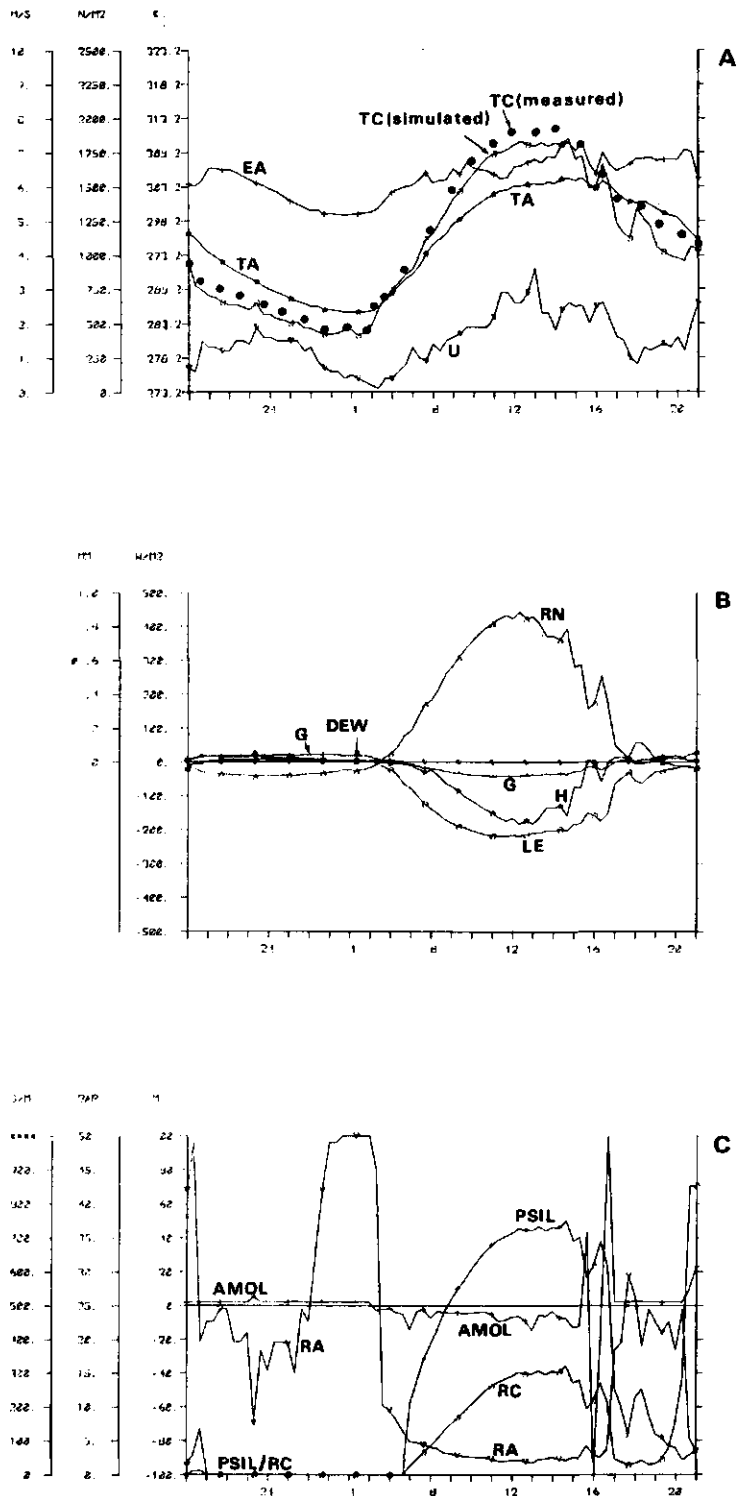
Fig. 18a, b and c. Model output for $\Psi_S = -350$ kPa

Table 5. Simulation results at 2-hour intervals from 2000 of 7 July to 2000 of 8 July 1975

fine sand: Ψ_s = -350 kPa

b = 0.10 m

b = 0.003 m

r_{pl} = 10 000 d

air pressure = 1.013 bar

Time	Input parameters:					Output parameters:								
	R_s	R_l	T_a	e_a	u	R_n	G	H	L.E	T_c	r_a	r_c	Ψ_l	Λ
	$W.m^{-2}$	$W.m^{-2}$	K	Pa	$m.s^{-1}$	$W.m^{-2}$	$W.m^{-2}$	$W.m^{-2}$	$W.m^{-2}$	K	$s.m^{-1}$	$s.m^{-1}$	bar	m
2000						- 16.7	12.0	8.9	- 4.1	288.6	980.5	57.9	- 0.6	-
2200						- 37.1	17.6	13.7	5.7	285.9	490.2	-	0	-
2400						- 41.4	18.4	14.6	8.7	284.5	305.9	-	0	2.4
200						- 36.2	21.0	8.8	6.4	282.5	452.5	-	0	-
400						- 23.7	18.6	2.8	2.3	282.3	1176.6	-	0	-
600		like table 4				24.5	0.8	- 3.1	- 22.6	288.1	190.0	-	0	-
800						183.1	-19.7	- 24.3	-139.1	296.3	79.8	82.0	- 19.2	7.4
1000						355.8	-37.8	-114.9	-203.2	305.1	51.9	206.5	- 30.3	4.4
1200						425.4	-41.6	-166.4	-217.4	309.3	42.4	290.1	- 35.7	7.0
1400						372.0	-35.1	-134.1	-203.1	309.5	51.1	304.5	- 36.5	7.0
1600						175.5	-13.5	- 4.1	-157.9	303.1	61.0	217.1	- 31.0	-181.7
1800						58.8	- 5.2	1.9	- 55.5	300.0	526.7	33.3	- 11.4	2.8
2000						- 11.0	10.8	19.4	- 19.1	292.7	367.7	156.5	- 4.0	-

At night the crop temperatures at dry soil are lower than those at wet soil. The outgoing longwave radiation flux must be compensated by an upward heat flux in the soil. When the soil is dry, the heat conductivity is low and the heat transport towards the crop surface is more difficult. This results in a lower crop temperature.

Fig. 17b and 18b show the energy balance components and the accumulated dew for wet and dry soil respectively.

By day, the heat flux into the soil (G) is relatively small compared to the net radiation flux. This heat flux touches in wet soil a value of -70 $W.m^{-2}$, in dry soil -42 $W.m^{-2}$. These differences are mainly due to differences in heat conductivity, but also to differences in heat capacity and surface temperature amplitude. At night the heat flux in wet soil touches 43 $W.m^{-2}$, that in dry soil 22 $W.m^{-2}$. The behaviour of the heat flux into the soil over the day is identical for wet and dry soil.

Fig. 19a and 19b show the simulated soil temperatures profiles at various times of the day for wet and dry soil respectively. Fig. 20a and 20b show the daily behaviour of the soil temperature at 0, -4 and -10 cm depth. For the dry soil, the simulated values at -4 cm depth are compared with measured values. The agreement is good. The amplitude of the measured values is somewhat larger.
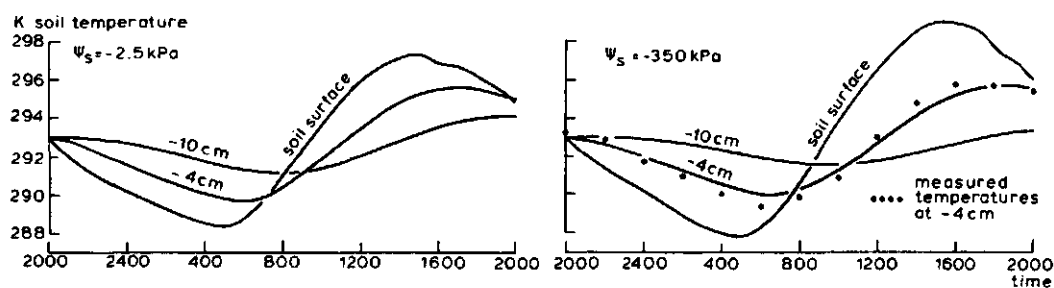
Fig. 19. Simulated soil temperature profiles for various times of the day for Ψ_s = -2.5 kPa(a) and for Ψ_s = -350 kPa(b)
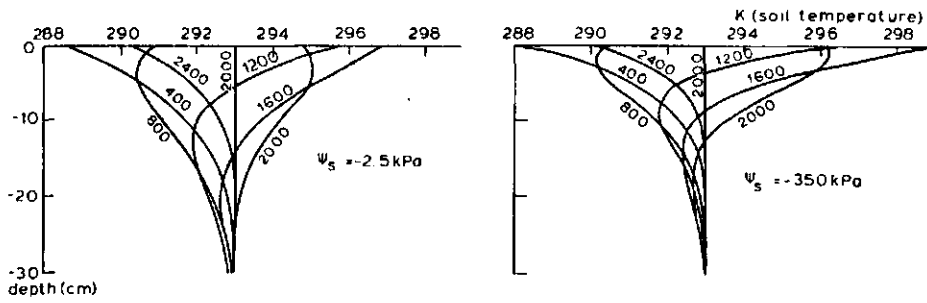
Fig. 20. Simulated daily behaviour of the soil temperature at 0. -4
and -10 cm depth for Ψ_s = -2.5 kPa(a) and Ψ_s = -350 kPa(b).
In fig. 20b, simulated values at -4 cm depth are compared
with measured values

By day, the net radiation flux (RN) is up to 40 $W.m^{-2}$ smaller for
the dry soil. This is due to higher crop temperatures, resulting in
more outgoing longwave radiation. At night, lower crop temperatures
at the dry soil result in higher net radiation values. For the dry
soil, simulated net radiation values are compared with measured
values (fig. 21). The agreement is rather good.
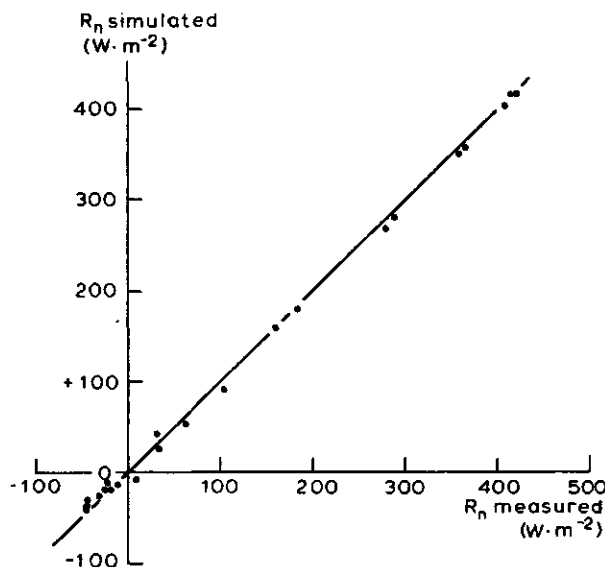
Fig. 21. Comparison between simulated and measured values of the net
radiation flux R_n

5. REFERENCES

BERGER, A., 1973. Le potentiel hydrique et la résistance à la diffusion dans les stomates indicateurs de l'état hydrique de la plante. Unesco, dans: Réponse des plantes aux facteurs climatiques, Actes Coll. Uppsala, 1970. 201-212.

BROOKS, R.H., and A.T. COREY, 1964. Hydraulic properties of porous media. Hydrology Paper No. 3, Colorado State University, Fort Collius, Colorado.

BRUNT, D., 1939. Physical and dynamical Meteorology, Cambridge University Press.

BRUTSAERT, W., 1977. Theory of evaporation in the Atmospheric Boundary Layer; not yet published. 167 pp.

BUSINGER, J.A., 1966. Transfer of momentum and heat in the planetary boundary layer, Proc. Symp. Arct. Heat Budg. and Atm. Circ., The RAND Corp., Santa Monica, Calif.: 305-322.

————— , J.C. WYNGAARD, Y. IZUMI and E.F. BRADLEY, 1971. Flux profile relationships in the atmospheric surface layer. J. Atm. Sci., 28: 181-189.

DYER, A.J., 1967. The turbulent transport of heat and water vapour in an unstable atmosphere. Quart. J. Roy. Meteorol. Soc., 93: 501-508.

FEDDES, R.A., 1971. Water, heat and crop growth. Comm. Agric. Univ., 71-12 (1971), Wageningen, The Netherlands. 184 pp.

————— and P.E. RIJTEMA, 1972. Water withdrawal by plant roots. Inst. for Land and Water Managem. Res., techn. bull. No. 83, Wageningen, The Netherlands. 59 pp.

HEILMAN, J.L., and E.T. KANEMASU, 1976. An evaluation of a resistance form of the energy balance to estimate evapotranspiration. Agron. J., 68: 607-611.

JONG, B. DE, 1973. Net radiation received by a horizontal surface at the earth. Delft University Press, Delft. 51 pp.

KALMA, J.D., and R. BADHAM, 1972. The radiation balance of a tropical pasture. I. The reflection of shortwave radiation. Agric. Meteorol., 10: 251-259.

LALIBERTE, G.E., R.H. BROOKS and A.T. COREY, 1968. Permeability cal-
culated from desaturation data. J. Irr. and Drain. Div.
A.S.C.E., 94: 57-71.

MONIN, A.S., and A.M. OBUKHOV, 1954. Dimensionless characteristics of
turbulence in the surface layer. Akad. Nauk. SSSR, Geofiz.
Inst., Tr., 24: 163-187.

MONTEITH, J.L., 1973. Principles of environmental physics. Edward
Arnold, London. 241 pp.

PAULSON, C.A., 1970. The mathematical representation of wind speed
and temperature profiles in the unstable atmospheric surface
layer. J. Appl. Meteorol., 9: 857-861.

RIJTEMA, P.E., 1965. An analysis of actual evapotranspiration. Agric.
Res. Rep. 659, Pudoc, Wageningen, 107 pp.

RIPLEY, E.A., and R.E. REDMANN, 1976. Grassland. In: J.L. Monteith,
Vegetation and the atmosphere, volume 2: Case studies. Acade-
mic Press, London. 351-398.

ROSEMA, A., (1975). A mathematical model for simulation of the termal
behaviour of bare soils, based on heat and moisture transfer.
NIWARS publ. No. 11, Delft, The Netherlands, 92 pp.

ROSS, J., 1975. Radiative transfer in Plant Communities. In: J.L.
Monteith, Vegetation and the Atmosphere, volume 1: Principles.
Academic Press. London. 13-55.

SHAWCROFT, R.W., E.R. LEMON and D.W. STEWART, 1973. Estimation of
internal crop water status from meteorological and plant
parameters. Unesco. Plant response to climatic factors. Proc.
Uppsala Symp., 1970. 449-459.

SMITHSONIAN METEOROLOGICAL TABLES, 1968. Sixth revised edition, pre-
pared by R.J. List. Smithsonian Instution Press, City of
Washington. 527 pp.

SOER, G.J.R., 1977. Estimation of regional evapotranspiration and
soil moisture conditions using remotely sensed crop surface
temperatures. NIWARS publication 45, Delft.

THOM, A.S., 1972. Momentum, Mass and heat exchange of vegetation.
Quart. J. Roy. Meteorol. Soc., 98: 124-134.

TURNER, N.C., 1973. Illumination and stomatal resistance to transpi-
ration in three field crops. Unesco. Plant response to clima-
tic factors. Proc. Uppsala Symp., 1970. 63-68.

VRIES, D.A. DE, 1952. Het warmtegeleidingsvermogen van grond. Meded.
    Landbouwhogeschool, Wageningen 52: 72 pp.
———   1975. Heat transfer in soils. In: D.A. de Vries and N.H. Afgan,
    Heat and mass transfer in the biosphere. Part 1: Transfer
    processes in the plant environment. Scripta book Company,
    Washington, D.C. 5-28.
WEBB, E.K., 1970. Profile relationships: The log-linear range, and
    extension to strong stability. Quart. J. Roy. Meteorol. Soc.
    96: 67-90.

```
C              . WIND VELOCITY AT ZA (U = M/S)
C
C-----------------------------------------------------------------
C
       DIMENSION RL(400),RS(400),TPA(400),EA(400),U(400)
       DIMENSION TPS(0/16),TPSNEW(15)
C
C   INPUT OF DATA
C   --------------
C
       OPEN(UNIT=1,ACCESS='SEQIN',FILE='TERGRA.DAT')
       READ(1,101)DATE,HOUR,AMIN,DELT,DT,DAYS,G
       READ(1,102)PSIS,THETAS,BL,SR,D,SO,AKO,PSIA,HCS,HCD,PSIDHC,CARIS
       READ(1,103)(TPS(J),J=1,16)
       READ(1,104)GHC,RPL,RD,DD,REFL,EC
       READ(1,105)TPO,PA,CTST,SLAT,DECL,ZR
       IT=DAYS*1440./DELT+1.
       DO 1 I=1,IT
          READ(1,106)RS(I),RL(I),TPA(I),EA(I),U(I)
    1    CONTINUE
  101    FORMAT(F6.0,4F5.0,2F7.3)
  102    FORMAT(F8.1,5F7.3/F8.4,F8.1,2F6.2,F8.1,F8.4)
  103    FORMAT(8F7.1/8F7.1)
  104    FORMAT(F6.2,F8.0,F5.1,F6.2,F7.3,F6.2)
  105    FORMAT(F7.1,F9.0,3F7.2,F6.2)
  106    FORMAT(F6.1,2F7.1,F7.0,F6.1)
       CLOSE(UNIT=1,FILE='TERGRA.DAT')
C
C   STATIC PART OF THE MODEL
C   ---------------------------
C
C
C      DETERMINATION PARAMETERS, CONSTANT DURING SIMULATION
C
       TPK=273.2
       RG=8.31432
       AMV=.0180153
       AMA=.0289644
       AKAR=.40
       ROWA=998.2
       PSILMI=-7E5
       PSILMA=-5E6
       Z=ZR-.67*GHC
       ZO=.13*GHC
       ALN=ALOG(Z/ZO)
       AKO=AKO/86400.
       CARIS=CARIS/86400.
       RPL=RPL*86400.
       RD=RD/1000.
       DTS=DT*60.
       PSIS=PSIS*1000.
       PSIA=PSIA*1000.
       PSIDHC=PSIDHC*1000.
C
C      CALCULATION INITIAL THETA VALUE
C
       PSIT=PSIS/PSIA
       SE=1./PSIT**BL
       S=SE*(1.-SR)+SR
       THETA=S*THETAS
C
```

```
               RFAC=.25*HCS/HC*RHOC/RHOCS
               AA=HC*DTS/RHOC/2/.02**2
               TPSNEW(1)=TPS(1)+AA*(RFAC*TPS(0)-(1.+RFAC)*TPS(1)+TPS(2))
               DO 10 J=2,15
                  TPSNEW(J)=TPS(J)+AA*(TPS(J-1)-2.*TPS(J)+TPS(J+1))
        10     CONTINUE
               GHF=.01*RHOC/DTS*(TPS(1)-TPSNEW(1))
               DO 11 J=2,15
                  GHF=GHF-.02*(TPSNEW(J)-TPS(J))*RHOC/DTS
        11     CONTINUE
               GHF=GHF-HC*(TPSNEW(15)-TPS(16))
        C
        C      - CALCULATION SENSIBLE HEAT FLUX
        C
               IF(TPAI.EQ.TPO) GO TO 21
               C1=TPAI*UI**2./G/(TPAI-TPO)
               IF(C1.GE.0.) GO TO 20
               AMOL=C1/ALN
               X=(1.-16.*Z/AMOL)**.25
               PSIONE=2.*ALOG((1.+X)/2.)+ALOG((1.+X**2.)/2.)-2.*ATAN(X)+
        1      1.570796
               PSITWO=2.*ALOG((1.+X**2.)/2.)
               RA=(ALN-PSIONE)*(ALN-PSITWO)/AKAR**2./UI
               GO TO 30
        20     AMOL=(C1-4.7*Z)/ALN
               IF(AMOL.LT.Z)AMOL=Z
               RA=(ALN+4.7*Z/AMOL)**2./AKAR**2./UI
               GO TO 30
        21     RA=ALN**2./AKAR**2./UI
        30     H=RHO*CP/RA*(TPAI-TPO)
        C
        C      - CALCULATION LATENT HEAT FLUX
        C
               PSICO=PSIL
               IF(DEW.GT.0.)PSICO=0.
               EOS=610.7*(273.15/(TPO-.05))**4.76696*EXP(24.606487*
        1      (TPO-TPK)/(TPO-.05))*EXP(AMV/RG/TPO*PSICO/ROWA)
               IF(EOS.LT.EAI.OR.DEW.GT.0.) GO TO 31
               PSIL=PSIS-(RPL+RD/AK)*(RNI+GHF+H)*G/ALABDA
               IF(PSIL.GT.PSIS) PSIL=PSIS
               IF(PSIL.LT.PSILMA) PSIL=PSILMA
               FP=ABS(PSIL)*.00001
               IF(FP.LE.ABS(PSILMI)*.00001) FP=ABS(PSILMI)*.00001
               RC=1./GHC**.5*(.05*FP**2.1+400./(RSI+1.5))
               GO TO 32
        31     RC=0.
        32     ALE=RHO*CP/GAMMA/(RA+RC)*(EAI-EOS)
        C
        C      - CHECK ON ENERGY BALANCE EQUATION
        C
               ENBA=RNI+GHF+ALE+H
               IF(ABS(ENBA).LT..5) GO TO 50
               IF(ENBA.GT.0.) TPL=TPO
               IF(ENBA.LT.0.) TPR=TPO
        40     CONTINUE
        50     DO 51 J=1,15
                  TPS(J)=TPSNEW(J)
        51     CONTINUE
        C
        C      CALCULATION WATER BALANCE/NEW SOIL MOISTURE PRESSURE
```

```
C     DYNAMIC PART OF THE MODEL
C     ----------------------------------
C
      DEW=0.
      PSIL=0.
      IP=0
C
C     CALCULATION METEOROLOGICAL BOUNDARY CONDITIONS
C
      ITIME=IFIX(DAYS*1440./DT+1.)
      OPEN(UNIT=20,ACCESS='SEQOUT',FILE='TER001.DAT')
      DO 80 I=1,ITIME
        ZONEST=HOUR+AMIN/60.
        TRUEST=ZONEST+CTST
        HOAN=(TRUEST-12.)*15.
        SUNEL=57.296*ASIN(SIND(SLAT)*SIND(DECL)+COSD(SLAT)*COSD(DECL)*
     1 COSD(HOAN))
        IF(SUNEL.LE.0.) SUNEL=0.
        DATIME=DT*FLOAT(I-1)
        AITT=DATIME/DELT+1.
        ITT=AITT
        RSI=RS(ITT)+(AITT-FLOAT(ITT))*(RS(ITT+1)-RS(ITT))
        RLI=RL(ITT)+(AITT-ITT)*(RL(ITT+1)-RL(ITT))
        TPAI=TPA(ITT)+(AITT-FLOAT(ITT))*(TPA(ITT+1)-TPA(ITT))
        EAI=EA(ITT)+(AITT-FLOAT(ITT))*(EA(ITT+1)-EA(ITT))
        UI=U(ITT)+(AITT-FLOAT(ITT))*(U(ITT+1)-U(ITT))
        IF(UI.LT..1) UI=.1
C
C     CALCULATION DYNAMIC CONSTANTS
C
      REFLEC=REFL/(1.+.6*SIND(SUNEL))
      CP=(1005.*(PA-EAI)+1850.*EAI)/PA
      RHOAIR=(PA-EAI)*AMA/RG/TPAI
      RHOVAP=EAI*AMV/RG/TPAI
      RHO=RHOAIR+RHOVAP
      ALABDA=2501000.-2200*(TPAI-TPK)
      GAMMA=CP*PA*AMA/AMV/ALABDA
      AKP=1./PSIT**(2.+3.*BL)
      AK=AKO*AKR
      HC=HCS-(HCS-HCD)*ALOG(PSIS/PSIA)/ALOG(PSIDHC/PSIA)
      RHOC=1.E6*((1.-THETAS-SO)*2.+SO*2.5+THETA*4.2)
C
C     ITERATION PROCEDURE
C
      TPL=TPO-.5*DT
      IF(TPL.LT.TPK)TPL=TPK
      TPR=TPO+.5*DT
      TPOR=TPO
      DO 40 M=1,11
        TPO=.5*(TPL+TPR)
C
C     - CALCULATION NET RADIATION
C
        RLO=EC*5.67E-8*TPO**4.
        RNI=(1.-REFLEC)*RSI+EC*RLI-RLO
C
C     - CALCULATION GROUND HEAT FLUX
C
        TPS(0)=TPO
        RHOCS=1.E6*((1.-THETAS-SO)*2.+SO*2.5+THETAS*4.2)
```

```
C
            EVAP=ALE*DTS/ALABDA/ROWA
            DEW=DEW+EVAP
            IF(DEW.LT.0.) DEW=0.
            IF(DEW.GT.0.) PSIL=PSIS
            SINK=(PSIL-PSIS)/(RPL+PD/AK)*DTS/ROWA/G
            THETA=THETA+SINK+CARIS/DD*DTS
            IF(THETA.GT.THETAS)THETA=THETAS
            IF(THETA.LT.SR*THETAS+.0001)THETA=SR*THETAS+.0001
            S=THETA/THETAS
            SE=(S-SR)/(1.-SR)
            PSIT=(1./SE)**(1./RL)
            PSIS=PSIT*PSIA
C
C     RESULTS ARE WRITTEN AT MOMENTS OF METEOROLOGICAL OBSERVATIONS
C
            IF(ABS(ITT-AITT).LE..00001) GO TO 60
            GO TO 61
   60       IF(AMOL.GT.999.) AMOL=999.
            IF(AMOL.LT.-999.) AMOL=-999.
            WRITE(20,201)RNI,GHF,H,ALE,UI,EAI,TPAI,TPO,PSIL,RC,RA,AMOL,
          1 DEW
  201       FORMAT(4F6.1,F4.1,F6.0,2F6.1,F10.1,2F7.1,F6.1,F8.5)
            WRITE(1,901)(TPS(J),J=1,16)
  901       FORMAT(16F6.1)
C
C     CHANGE OF TIME
C
   61       AMIN=AMIN+DT
            IF(AMIN.GE.60.)GO TO 62
            GO TO 63
   62       AMIN=AMIN-60.
            HOUR=HOUR+1.
   63       IF(HOUR.GE.24.) GO TO 64
            GO TO 80
   64       HOUR=HOUR-24.
            DATE=DATE+1.
   80       CONTINUE
            CLOSE(UNIT=20,FILE='TER001.DAT')
            END
```